An Algorithm for the Detection and Tracking of Tropical Mesoscale Convective Systems Using Infrared Images From Geostationary Satellite

Thomas Fiolleau, Rémy Roca

▶ **To cite this version:**

Thomas Fiolleau, Rémy Roca. An Algorithm for the Detection and Tracking of Tropical Mesoscale Convective Systems Using Infrared Images From Geostationary Satellite. IEEE Transactions on Geoscience and Remote Sensing, 2013, 51 (7), pp.4302-4315. 10.1109/tgrs.2012.2227762 . hal-00996334

HAL Id: hal-00996334
https://hal.science/hal-00996334v1

Submitted on 29 Jul 2022

HAL is a multi-disciplinary open access archive for the deposit and dissemination of scientific research documents, whether they are published or not. The documents may come from teaching and research institutions in France or abroad, or from public or private research centers.

L'archive ouverte pluridisciplinaire **HAL**, est destinée au dépôt et à la diffusion de documents scientifiques de niveau recherche, publiés ou non, émanant des établissements d'enseignement et de recherche français ou étrangers, des laboratoires publics ou privés.

This article has been accepted for inclusion in a future issue of this journal. Content is final as presented, with the exception of pagination.

An Algorithm for the Detection and Tracking of Tropical Mesoscale Convective Systems Using Infrared Images From Geostationary Satellite

Thomas Fiolleau and Rémy Roca

***Abstract*—This paper focuses on the tracking of mesoscale convective systems (MCS) from geostationary satellite infrared data in the tropical regions. In the past, several automatic tracking algorithms have been elaborated to tackle this problem. However, these techniques suffer from limitations in describing convection at the "true" scale and in depicting coherent MCS life cycles (split and merge artifacts). To overcome these issues, a new algorithm called Tracking Of Organized Convection Algorithm through a 3-D segmentatioN has been developed and is presented in this paper. This method operates in a time sequence of infrared images to identify and track MCS and is based on an iterative process of 3-D segmentation of the volume of infrared images. The objective of the new tracking algorithm is to associate the convective core of an MCS to its anvil cloud in the spatiotemporal domain. The technique is applied on various case studies over West Africa, Bay of Bengal, and South America. The efficiency of the new algorithm is established from an analysis of the case studies and via a statistical analysis showing that the cold cloud shield defined by a 235-K threshold in the spatiotemporal domain is decomposed into realistic MCSs. In comparison with an overlap-based tracking algorithm, the analysis reveals that MCSs are detected earlier in life cycle and later in their dissipation stages. Moreover, MCSs identified are not anymore affected by split and merge events along their life cycles, allowing a better characterization of their morphological parameters along their life cycles.**

***Index Terms*—Convective systems, meteorology, tracking, tropical regions.**

I. Introduction

OVER the intertropical belt, the water and energy cycle is strongly modulated by individual storm events embedded in the synoptic circulations like monsoons, waves, and intertropical convergence zone (ITCZ) [38]. Understanding the water and energy budget hence requires documenting these highly contributing storms. Deep cloud systems are spanning a wide range of scales and degree of organization in the tropics [35]. As a result, over the years, a rich terminology has been developed ranging from the mesoscale convective complex [26] and disturbance- or squall-line systems [2] to the organized convective systems [32] and the organized tropical storms and cyclones [41] or the super clusters [30] and other convective cloud clusters [43]. The commonality of all these definitions is that mesoscale cloud systems are composed of a convective core where heavy rainfall takes place at a typical scale of 10–100 km, associated to a stratiform anvil with lighter precipitation as well as nonprecipitating cirriform cloudiness of a typical scale of 100–1000 km (e.g., [36]) which we will refer to loosely in the rest of this paper as mesoscale convective systems (MCSs). The MCSs are further characterized by a life cycle, idealized in three stages: initiation, maturity, and a decaying phase where the ratio of the convective core and the stratiform anvils evolves in time [18].

While most of our understanding of the MCS arises from ground radar and *in situ* measurements (e.g., [8], [17], [19], [28]), satellite observations of these storms began very early in the history of satellite meteorology (e.g., [38] for an historical account). The first satellite pictures indeed reveal large cluster of organized cloudiness all over the tropics. First, animated series of images from geostationary orbit further showed that these cloud patches were evolving in time, moving, and dissipating. Since then, infrared imagery from geostationary satellite has been heavily used to document some aspects of the morphology of the MCSs.

Up to the mid 1980s, MCSs were identified and tracked manually [2], [7], [31]. These pioneering studies yield interesting information on the evolution of the cold cloud shield life cycle in links with the meteorological conditions [3]. Automatic tracking algorithms have then been proposed to overcome the limitations of the manual identification (small data set, sensitivity of the results to the operator, etc.). In this paper, we present one such automatic algorithm to detect and track in time the tropical MCS from infrared image series acquired from a geostationary platform. The new algorithm is based on an original 3-D image processing approach and is named Tracking Of Organized Convection Algorithm through a 3-D segmentatioN (TOOCAN).

This paper is organized as follows. First, a quick review of existing methods and their limitations is provided. Section III presents the functioning of the TOOCAN algorithm. Section IV is devoted to the analysis of the results of the segmentation technique, while Section V is focused on the evaluation of the TOOCAN's outputs. A summary and discussion section ends this paper.

Manuscript received March 30, 2012; revised September 4, 2012; accepted September 23, 2012. This work was supported in part by Centre National d'Etudes Spatiales (CNES) and in part by Centre National de la Recherche Scientifique (CNRS).

T. Fiolleau was with the Laboratoire de Météorologie Dynamique, Institut Pierre et Simon Laplace, 75252 Paris, France. He is now with the Centro Nacional De Monitoramento e Alertas de Desastres Naturais (CEMADEN), 12630-000 Cachoeira Paulista, Brazil (e-mail: thomas.fiolleau@cptec.inpe.br).

R. Roca was with the Laboratoire de Météorologie Dynamique, Institut Pierre et Simon Laplace, 75252 Paris, France. He is now with the Laboratoire d'Etudes en Géographie et Océanographie Spatiales, 31401 Toulouse, France (e-mail: remy.roca@legos.obs-mip.fr).

Color versions of one or more of the figures in this paper are available online at http://ieeexplore.ieee.org.

Digital Object Identifier 10.1109/TGRS.2012.2227762

0196-2892/$31.00 © 2013 IEEE

This article has been accepted for inclusion in a future issue of this journal. Content is final as presented, with the exception of pagination.

II. Quick Review of MCS Detection and Tracking Algorithms

The MCS detection and tracking algorithms aim at providing for each individual convective system the following morphological characteristics: size of the cloud shield, minimum brightness temperature, propagation speed, and their evolutions along the life cycle of the storm. The automatic tracking algorithms are generally based on two stages (e.g., [45]).

1) A detection stage aiming at identifying the convective clusters in the infrared geostationary imagery at a given time. It consists in applying threshold clustering techniques to delineate the cold cloud shield associated with the convective clusters.
2) A tracking stage linking convective clusters from one image to the next in order to build the convective system all along its life cycle.

The detection stage has not received much attention since the earliest time and usually consists simply in a thresholding of the infrared images using a cold brightness temperature threshold to delineate continuous areas of deep convective cloudiness. The selection of the threshold spans a wide range depending upon the analysis, typically ranging from 208 K to 255 K [27], [29], [30]. In a meteorological perspective, adaptative thresholds have been used to detect convective cells according to their vertical extent in their earlier initiation stages [34]. A notable effort to go beyond this simple detection is the detect-and-spread method (DAS), an iterative multithreshold approach [4]. This technique, operating in multiple steps, delineates the whole cloudy area (convective core and stratiform anvil) in two dimensions within a geostationary satellite image. It has been tailored in the tropics to the upper-level cloud defined with a bold threshold in the infrared image [36] and successfully used in conjunction with a multispectral cloud classification scheme [37]. At a given threshold, the DAS technique tends to produce smaller clusters than the use of simpler techniques. Innovative methods have recently been developed to improve the detection of MCSs. Thus, Shukla and Pal in [40] have elaborated an algorithm based on a source apportionment technique to detect and nowcast MCSs. To deal with the highly deformable nature of convective clouds, techniques using implicit curve descriptor, known as the level set method, have also been developed to detect and track convective cells [42].

On the other hand, the tracking stage has seen relatively much more creative algorithm developments. Several tracking algorithms have been indeed elaborated based on a minimization of a cost function using the distance and the area difference between convective clusters in successive images [15], [16], on a maximum spatial correlation tracking technique [6], [9], [10], on a projected centroid location [21], on a greedy optimization of position error and longevity [23], and on a checking overlap followed by a global cost function [14]. However, the most used methodology in the community remains the "area-overlapping" technique. This method is based on the geographical overlapping between convective clouds on two consecutive images [1], [45]. If the overlap is greater than 50% or 10 000 km^2 of the area of either the current cluster or the cluster from the previous image, convective clusters are matched and linked. Cloud system is considered to generate when no overlapping occurs in the previous image. On the other hand, a convective system dissipates when there is no longer intersection with another cluster in the next image. When multiple clusters are found at one of the steps, the matching with the single cluster gives rise to some cluster merging and splitting. Some criterion on the size of the cluster and on the overlap area is used to connect the singleton to its mother cluster or its infant clusters. These issues yield complex MCS life cycles and perturb the documentation of the physical life cycle of the convective systems. To overcome these tracking issues, preprocessing operations such as quality control and morphological operations [14] have been suggested to improve the trackability of storms. However, whatever the tracking technique used, unphysical splitting/merging of the clusters within the life cycle of the MCS remains a problem that strongly limits the usage of MCS detection and tracking results (for instance, see [44] in the meteorological forecast framework [22]).

These detection and tracking issues prompted us to elaborate a new automatic tracking algorithm in order to improve the characterization of the MCSs whatever their degrees of organization in the space and time domains. This new algorithm can be seen as an extension of the original DAS technique to operate in three dimensions within a spatiotemporal volume of infrared images (instead of a 2-D image). In line with previous studies, in the following, a single threshold of 235 K is applied on temporal series of geostationary infrared images in order to delineate the upper-level cloudiness volume associated with deep convective cloudiness.

III. TOOCAN Algorithm

A. Cluster Distribution in the Geostationary Infrared 3-D Imagery

Before introducing the 3-D segmentation operated by the TOOCAN algorithm, it is necessary to analyze the impact of various brightness temperature thresholds on the area and lifetime of cloud clusters. For this, a set of infrared images are segmented using five different brightness temperature thresholds (190 K, 200 K, 210 K, 220 K, and 235 K). Three-dimensional clusters are defined as a contiguous area of pixels with a brightness temperature lower than the threshold in the spatiotemporal domain. Fig. 1(a) shows the normalized cumulated distribution of the population of these clusters. The resemblance of the distributions of population segmented by thresholds within the range 200 K–235 K indicates that there is a small dependence of the cluster volume to the temperature thresholds. Fifty percent of the clusters are due to those exhibiting a volume lower than ten pixels in the three dimensions. However, for a brightness temperature threshold of 190 K, 3-D clusters smaller than three pixels explain 50% of the population. Note that no clusters segmented by the 190-K threshold reach a volume larger than 500 pixels. Fig. 1(b) shows the normalized cumulated contribution to the total cold cloudiness according to the cluster volumes and for the same temperature thresholds. Contrary to the distribution of population, the contribution of the cold cloudiness appears sensitive to the temperature thresholds. Thus, 50% of the cold cloudiness is due to clusters larger than 350 pixels for

This article has been accepted for inclusion in a future issue of this journal. Content is final as presented, with the exception of pagination.

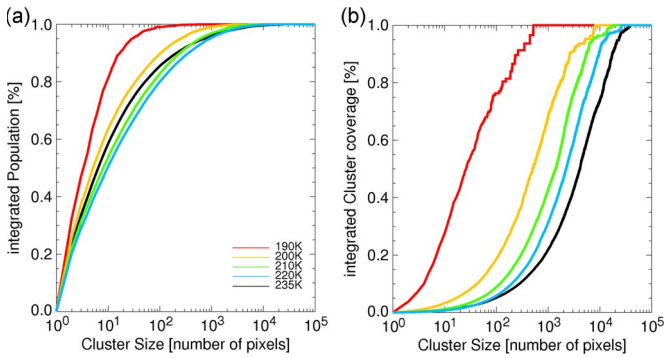

Fig. 1. (a) Normalized cumulated distribution function of the 3-D-cluster occurrence as a function of the cluster volume (in pixels). (b) Normalized cumulated contribution of the 3-D-cluster occurrence weighted by cold cloudiness as a function of the cluster volume (in pixels). Statistics are computed for the period of July 2006 over West Africa, and the imagery is segmented with different brightness temperature thresholds indicated by colors.

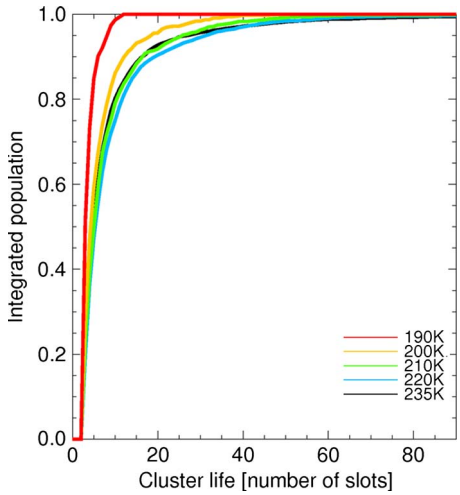

Fig. 2. Normalized cumulated distribution function of the 3-D-cluster occurrence as a function of the cluster lifetime duration (in slot). Statistics are computed for the period of July 2006 over West Africa, and the imagery is segmented with different brightness temperature thresholds indicated by colors.

a 200-K threshold, whereas half of the total cluster coverage defined at 235 K is explained by clusters larger than 2100 pixels in the spatiotemporal domain.

Fig. 2 shows the normalized cumulated distribution function of the cluster population, according to their lifetime durations. The distributions reveal that 50% of the clusters segmented by thresholds within the range 200 K–235 K are due to systems with lifetime shorter than five frames. Within this range, the cluster lifetime durations seem to be insensitive to the temperature threshold. However, for a threshold of 190 K, clusters lasting less than three frames explain more than 50% of the population. No cluster segmented by a 190-K threshold lasts more than 12 frames. In the following, these observations will be used to specify the volume and the minimum lifetime criteria used in the TOOCAN algorithm.

B. Functioning of the TOOCAN Algorithm

In order to develop an automated algorithm dedicated to the identification and the tracking of MCS, it is necessary to introduce a simple definition of an MCS encountered whatever

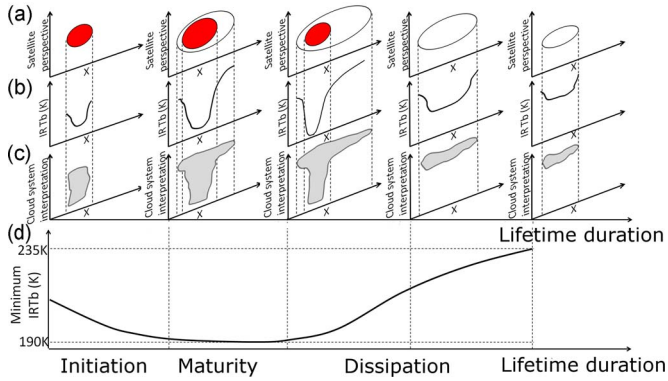

Fig. 3. (a) Scheme of the evolution of an MCS for successive time steps and from satellite perspectives. Red part corresponds to the convective core, while the black line represents the high cold cloud shield boundaries. (b) Minimum brightness temperature in an X cross section for the successive time steps of the life cycle. (c) Associated convective system for the successive time steps of the life cycle. (d) Minimum brightness temperature along the MCS life cycle.

the degree of organized convection which takes place over the tropical regions. For this study, an MCS is thus defined as a convective core with a cold brightness temperature associated to a stratiform part with a warmer brightness temperature in the spatiotemporal domain [17]. Fig. 3 shows a schematic of such a definition from a satellite perspective. With respect to this definition, the objective of the new tracking algorithm is thus to detect convective cores within a cold cloud shield and to associate them to their corresponding anvil clouds in the spatiotemporal domain. That way, the deep convective cloudiness, or the cold cloud shield, identified by a given brightness temperature threshold, is decomposed in several MCSs in the spatiotemporal domain. The DAS algorithm [4] gives us a basis to elaborate this new algorithm. This methodology is based on an image processing technique called region growing [33], [39]. The DAS algorithm relies on a clustering technique which progresses from the convective cores to the cloud edges, with the assumption that adjacent pixels in a satellite image belong to the same system and that the optical depth of the cloudiness decreases away from the convective core to the cloud edges [Fig. 3(b)].

This is for the spatial domain. Similarly, in the temporal domain, the optical depth decreases (and brightness temperatures increase) from the convective core to the cloud edges [Fig. 3(d)], and so, adjacent pixels in a volume image are assumed to belong to the same MCS. That way, the TOOCAN algorithm, by applying multisteps of detection and spread of convective seeds in the spatiotemporal domain can identify and characterize with consistency the MCSs all over their life cycles.

The new tracking algorithm then works in a time sequence of infrared images to identify and track MCSs not any more with the traditional detection and tracking steps but in a single 3-D (spatial+time) segmentation step. For this purpose, a spatiotemporal image, whose spatial axes are longitude and latitude, is generated by the time series of infrared images derived from geostationary satellites. The region growing technique requires the input of several seeds lower than a given brightness temperature threshold, which will be grown in the spatiotemporal domain to form the final regions, corresponding to the MCSs. Convective seeds are then first detected within

This article has been accepted for inclusion in a future issue of this journal. Content is final as presented, with the exception of pagination.

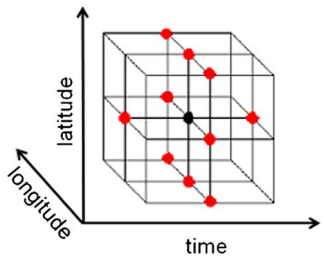

Fig. 4. Illustration of the ten-connectivity morphological operator used to dilate cloudy pixels in the spatiotemporal domain, eight-connectivity for a dilatation in the spatial domain and two-connectivity for a dilatation in the temporal domain.

the spatiotemporal volume and then spread until reaching the boundaries of the cold clouds. Thus, owing to this 3-D segmentation, MCSs can be characterized along their life cycles and fit the definition given previously. To decompose the total cold cloud shield, the TOOCAN algorithm is based on an iterative process of detection and growing of seeds at different temperature thresholds, so that various MCSs with various depths and brightness temperatures can be identified.

The main stages are the following.

1) A 3-D detection of individual convective seeds is performed in the spatiotemporal domain. It involves finding contiguous set of pixels whose temperature is colder than a given threshold and which has not been assigned to other already identified seeds. Each newly detected seed receives a unique label.
2) A 3-D identification of an intermediate cold cloud shield mask at a 5-K warmer threshold.
3) A spread of the convective seeds, in the spatiotemporal domain, to the cold cloud shield intermediate boundaries identified in the second stage. It involves adding edge pixels belonging to the cold cloud shield mask to all already identified seeds. During the spread stage, the dilatation of each pixel is constrained by a criterion on the brightness temperatures. The difference of brightness temperatures between the edge pixel and the current pixel has to be greater than a threshold set here at 1 K. This criterion permits the computation with a minimum of error the new boundaries of the seeds but also minimizes the effects of local minima encountered within a convective seed. Thus, all pixels in the feature domain are labeled by determining to which seed they belong.

A ten-connected spatiotemporal neighborhood is used for the region growing step (Fig. 4): eight-connected spatial neighborhood and two-connected temporal neighborhood (past and future), in order to emphasize the pixel dilatation in the spatial domain. A 190-K threshold is applied for the initial detection of the convective seeds, while a 195-K threshold is used to first identify the cold cloud shield boundaries. The iterative process then works with a 5-K detection step (Δ_{BT}) and is stopped when the cold cloud shield boundaries reach the 235-K brightness temperature threshold. The TOOCAN algorithm relies on two main parameters.

1) A lifetime threshold applied in the 3-D detection step, corresponding to the minimum duration allowed for a convective system to last. The lifetime threshold has been established to three images in order to describe MCSs trough their entire life cycles, from their initiation stages to their dissipation stages. Using this criterion, between 70% and 80% of the convective systems are segmented for thresholds in the range 200 K–235 K (Fig. 2). For 190 K, Fig. 2 shows that such a lifetime threshold permits a segmentation of 50% of the population of MCSs.
2) A volume threshold is also applied in the 3-D detection step in order to filter the convective seeds before spreading them to the cold cloud shield boundaries. The value of this threshold has been set to 75 pixels in the spatiotemporal domain (25 pixels per frame). According to Fig. 1(a), between 40% and 55% of the population of convective seeds have an area larger than 75 pixels in the three dimensions for a temperature threshold within the range 200 K–235 K. These systems contribute to more than 90% of the total cold cloudiness [Fig. 1(b)].

IV. First Results and Sensitivity Study

A. Case Study of West Africa

The September 11, 2006, over the region of Niamey has been selected for a case study of convective system identification and tracking. The data from METEOSAT second generation (MSG-1) in the 10.8-μ channels (3 km/15 min) are used for the analysis. The meteorological and cloud conditions are discussed at length in [5].

This convective situation is processed in the spatiotemporal domain by applying single brightness temperature thresholds in the time sequence of infrared images as well as by the TOOCAN algorithm. A comparison is then performed between the segmentation operated by TOOCAN for various steps of the iterative process and a simple segmentation of the cold cloud shield by single brightness temperature thresholds (Fig. 5). The results are shown for a single time step at 1600 UTC (Coordinated Universal Time). At a 205-K step, we can observe that the segmentation by a single threshold delineates four convective clusters. According to the TOOCAN intermediate outputs, at the same temperature threshold, five convective clusters have been identified. For a 220-K brightness temperature threshold, the segmentation by a single threshold gives rise to only two convective clusters, whereas the TOOCAN algorithm decomposed the convective cold cloud shield defined at 220 K into six convective clusters. Finally, we can observe that a segmentation of the convective situation by a single temperature set at 235 K gives rise to only one cluster. On the contrary, the cold cloud shield defined at 235 K is decomposed in several convective clusters by the TOOCAN algorithm. Fig. 5 shows that the TOOCAN methodology segments the infrared image in terms of individual convective systems, including core and anvil defined by the 235-K brightness temperature threshold. It also shows that a single 235-K threshold applied on the infrared imagery just identifies a cold cloud shield but does not describe with details the organization of the convection, unlike the segmentation performed by the TOOCAN algorithm which is more representative of the spatial scale of the organized convection.

This article has been accepted for inclusion in a future issue of this journal. Content is final as presented, with the exception of pagination.

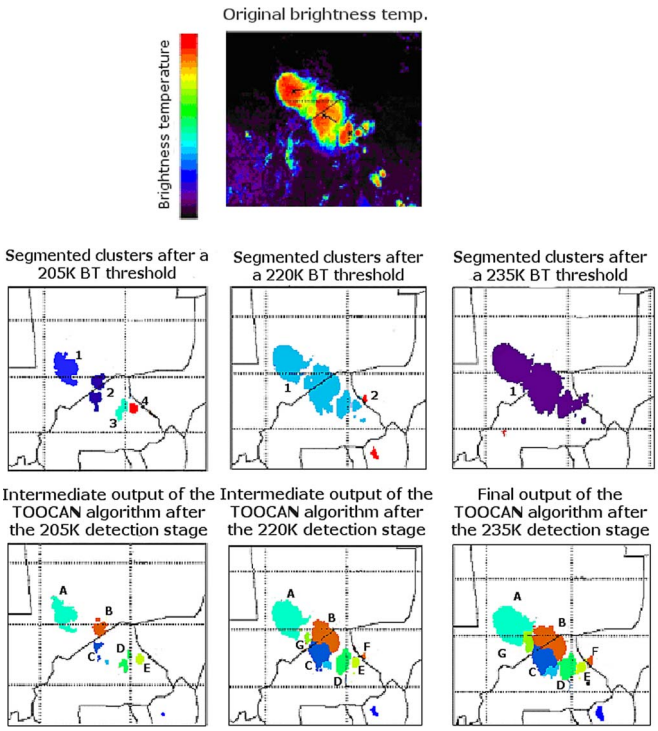

Fig. 5. (From top to bottom) Brightness temperature image at 1600 UTC in September 11, 2006, segmented clusters after 205-K, 220-K, and 235-K temperature thresholds, and intermediate outputs of the TOOCAN algorithm after the 205-K, 220-K, and 235-K detection stages.

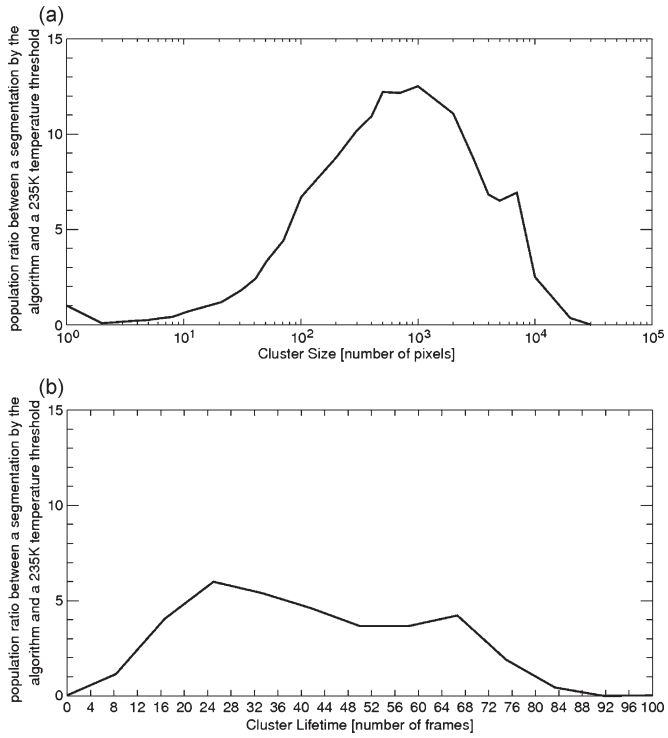

Fig. 6. (a) Population ratio between 3-D clusters segmented by the TOOCAN algorithm and 3-D clusters segmented by a single threshold set at 235 K for the July 2006 period, as a function of the cluster volumes and (b) as a function of the lifetime durations.

B. Statistical Analysis

The statistical behavior of the TOOCAN segmentation is evaluated by processing the whole month of July 2006 over the West African region. This corresponds to 353 000 clusters and around 17 500 convective systems. Fig. 6(a) shows the ratio of population of MCSs (in this section, MCSs are called 3-D convective clusters for a simplification) identified by the TOOCAN algorithm to the population of 3-D convective clusters segmented by a single threshold set at 235 K as a function of the cluster volumes and binned into classes. For clusters smaller than 20 pixels, the number of 3-D convective clusters segmented by the 235-K threshold is larger than those segmented with the TOOCAN algorithm in the spatiotemporal domain. This observation is inherent to the filtering of the 3-D convective clusters lower than 75 pixels in the 3-D detection steps of the TOOCAN algorithm.

For cluster volumes within the range 20 pixels–20 000 pixels, the distribution shows a larger population of 3-D convective clusters segmented by the TOOCAN methodology. The maximum of ratio is reached for the class [1000 pixels–2000 pixels] with up to 12 times more clusters segmented by the TOOCAN algorithm than with the single 235-K threshold. For the 3-D convective clusters larger than 20 000 pixels, the ratio of population indicates a larger number of clusters segmented by the 235-K threshold, explained by the fact that large cold cloud patches are sliced up in several convective systems by the TOOCAN algorithm.

Fig. 6(b) shows that, for clusters lasting less than eight images, the population of 3-D convective clusters segmented by a single 235-K threshold is larger than those identified with the TOOCAN algorithm. On the contrary, for cluster lifetimes within the range 8 images–72 images, the distribution shows a larger population of 3-D convective clusters segmented by the TOOCAN methodology. The maximum of ratio is reached for the class [24 images–28 images] with up to six times more clusters segmented by the TOOCAN algorithm than with the single 235-K threshold.

C. Sensitivity of the Cold Cloud Shield Segmentation by the TOOCAN Algorithm to the Detection Step

The volume threshold and the minimum lifetime criteria being set respectively to 75 pixels and 3 images, the sensitivity of the TOOCAN algorithm is then evaluated according to the value of the detection step criteria (Δ_{BT}). Fig. 7 shows the tracking scheme output over a selection of images at 1300 UTC, 1600 UTC, 1900 UTC, and 2100 UTC for this convective situation. The second row represents the clusters segmented by a single threshold set at 235 K, whereas the last three rows illustrate the outputs of the TOOCAN tracking for three different detection steps (2 K, 5 K, and 10 K). The sensitivity of the TOOCAN segmentation to Δ_{BT} is now evaluated. The segmentation of the cold cloud shield defined at 235 K by the new algorithm seems to be insensitive to Δ_{BT}. Indeed, large clusters seem to be detected similarly whatever the magnitude of the detection step used. However, we can observe that the greater the detection step, the smaller the number of detected MCSs is. A 2-K Δ_{BT} identifies 41 convective systems, a 5-K Δ_{BT} identifies 32 convective systems, and a 10-K Δ_{BT} segments 26 systems.

This article has been accepted for inclusion in a future issue of this journal. Content is final as presented, with the exception of pagination.

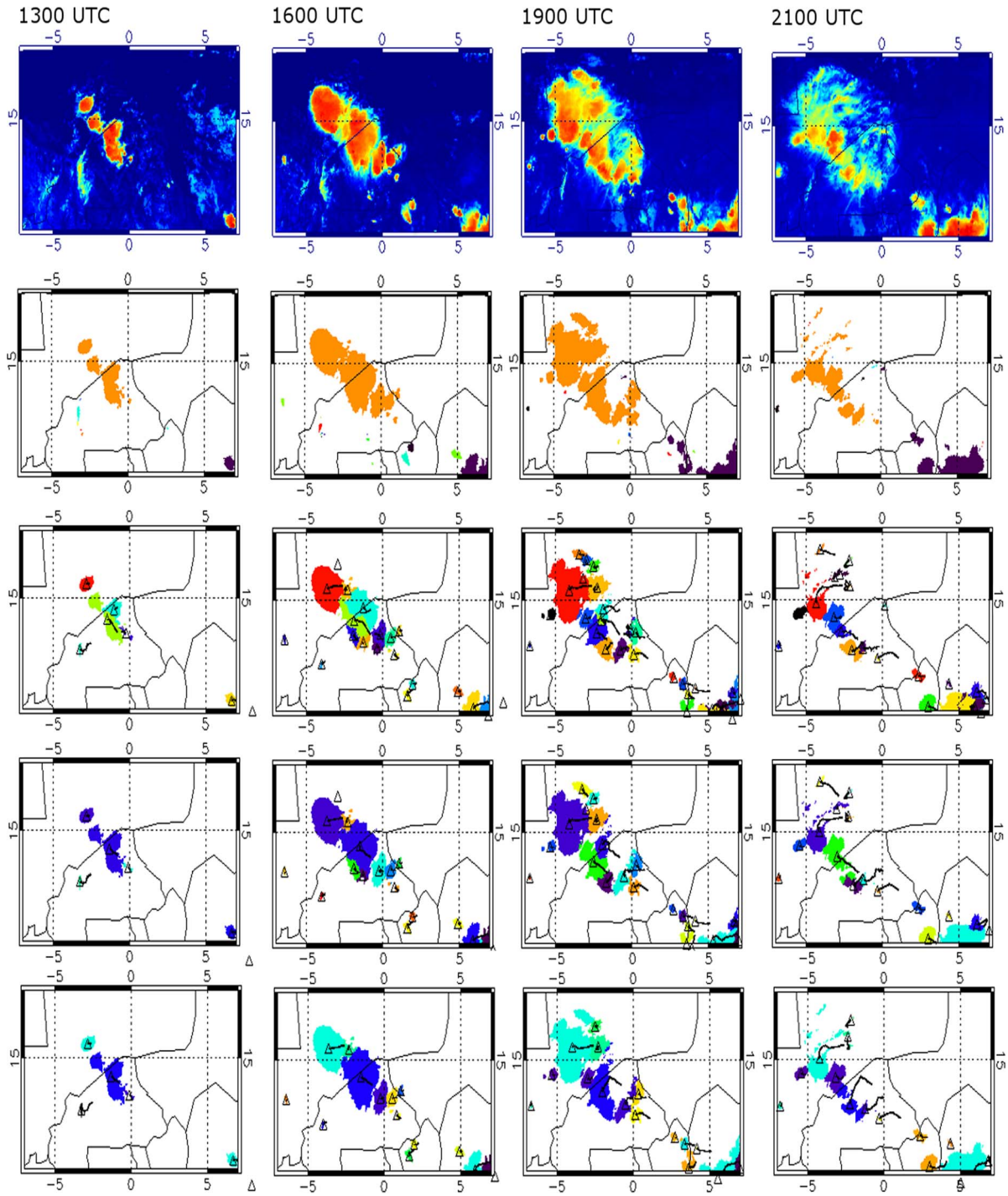

Fig. 7. Illustration of the sensitivity of the TOOCAN segmentation to the detection step criteria (Δ_{BT}) for a convective situation which occurred in September 11, 2006, over the region of Niamey. (From top to bottom) Time series of the Spinning Enhanced Visible and InfraRed Imager (SEVIRI)/MSG-1 brightness temperature images, time series of images segmented by using a single brightness temperature threshold set at 235 K, and time series of images processed by the TOOCAN tracking algorithm for a 2-K step, a 5-K step, and a 10-K step.

As noticed previously, during the spread stage, an adjacent pixel is associated to a convective seed, only if the difference of its brightness temperature with that of the current pixel is greater than 1 K. This criterion implies that, for a similar convective seed detected whatever the values of Δ_{BT} (2 K, 5 K, or 10 K), the final segmentation of the MCS will be similar at the end of the spread step. Thus, a Δ_{BT} of 2 K or 10 K segments a similar population of convective seeds, implying a similar segmentation of the corresponding MCSs. The convective seeds of large MCSs are detected whatever the detection step used, and so, the shape of these MCSs is pretty much the same at the end of the iterative process. A lower Δ_{BT} refines the segmentation of infrared imagery by detecting convective seeds corresponding to small MCSs, which cannot be detected with a larger Δ_{BT}. Thus, these additionally detected convective seeds involve a different aggregate of unallocated pixels during the spreading stages. A process of TOOCAN with small values of Δ_{BT} then allows a better precision in the characterization of

This article has been accepted for inclusion in a future issue of this journal. Content is final as presented, with the exception of pagination.

convection but does not affect the general characteristics of the larger MCSs, well identified whatever the value of Δ_{BT}.

For the following, Δ_{BT} is set at 5 K. Indeed, for long periods of study and regions, a 2-K detection step requires significantly long processing time, while a 5-K detection step gives rise to a coherent segmentation of the convection whatever its degree of organization, with reasonable processing time.

V. Comparison With a Tracking Algorithm Based on the "Area-Overlapping" Technique

The subjectivity inherent to the tracking of MCSs enhances the difficulty to evaluate and to validate a new tracking algorithm. However, it is important to estimate its capacity to segment MCSs as defined previously and then to have a measure of its efficiency. Several techniques have been promoted for this purpose. By creating a short-term forecast from the tracking algorithms, Lakshmanan *et al.* [23] and Han *et al.* [14] evaluate the storm-tracking algorithms by comparing the short-term forecast with current data. However, since the nowcasting is computed from the tracking algorithm, this method is an indirect measure of storm-tracking effectiveness. Some other methods compute a "percent correct" of cluster associations in a sequence of images, by comparing the automated tracking of cells with a human tracking [21]. However, this technique is time consuming, and moreover, the automatic tracking algorithm cannot be evaluated on large data sets. Lakshmanan and Smith in [25] evaluate different tracking algorithms by computing a composite skill score based on three factors: the lifetime duration of the track, the linearity of the track, and the preservation of a storm attribute. For our study, the evaluation of the effectiveness of the TOOCAN algorithm is based on comparing its results with those of a tracking algorithm based on a detection step by a single 235-K brightness temperature threshold and on a tracking step using an "area-overlapping" technique [32]. In order to evaluate the TOOCAN algorithm on MCSs characterized by different convective organization, an analysis of various case studies is performed over three tropical regions, two over continental regions (West Africa and South America) and one over an oceanic region (Bay of Bengal). These three case studies will allow us to measure the capability of the TOOCAN algorithm to segment MCSs over the whole tropical region. The West African case study, which occurred in September 11, 2006, over Niamey, will be discussed in more details. To complete the evaluation, a statistical analysis of the both algorithms is performed for the whole month of July 2006 over the West African region.

A. Case Studies

1) West Africa: Fig. 8 shows the tracking schemes over a selection of images at 1200 UTC, 1300 UTC, 1530 UTC, 1800 UTC, 2000 UTC, and 2030 UTC for the convective situation which occurred over the region of Niamey on September 11, 2006.

This figure illustrates the segmentation of MCSs by the new tracking method compared to the "area-overlapping" technique. First of all, we can observe subjectively that the new tracking algorithm identifies and tracks MCSs much as one would do from viewing the infrared images. The TOOCAN algorithm identifies 32 MCSs (five for the "area-overlapping" technique) for this period, from which none initiates by splitting or dissipates by merging (two splitting or merging events for the "area-overlapping" technique). The results of the "area-overlapping" algorithm show that no convective clusters have been identified in the first image at 1200 UTC. The "area-overlapping" algorithm then detects two convective clusters at 1300 UTC. However, between 1530 UTC and 2000 UTC, the MCS no. 2 is ended up by merging into the large cluster no. 1. Between 2000 UTC and 2030 UTC, a part of MCS no. 1 splits and gives rise to a new system (MCS no. 3). If one considers the MCS A processed by the TOOCAN algorithm, one can observe that this MCS initiates at 1200 UTC and consists in cluster 2 at 1300 UTC, a part of cluster 1 at 1530 UTC, 1800 UTC, and 2000 UTC and a part of cluster 3 at 2030 UTC. At 1300 UTC, the shape and area of MCS A are similar to MCS no. 2 processed by the "area-overlapping" technique. Indeed, at this time step, MCS no. 2 is a single and isolated MCS, whose area is greater than 5000 km^2 and which is composed from a unique convective core associated to a stratiform anvil. For this convective situation, a segmentation performed by TOOCAN is then equivalent to a technique identifying MCSs with a single 235-K threshold applied on the infrared imagery. Fig. 8 also reveals that the TOOCAN algorithm, owing to its independence from a minimum size criterion, is able to detect convection very early in its triggering stage (MCSs A, B, and C) and very late in its dissipation stage (MCSs F, G, and C). For example, MCS A is identified at 1200 UTC, 1 h (i.e., four images) before the detection of any cluster by the "area-overlapping" technique. This capability to detect convection very early is of utmost importance in a perspective of forecast applications. The observation of MCS A then shows us that the TOOCAN algorithm is able to manage complex convective situations by suppressing unphysical split and merge events due to tracking algorithm. Fig. 8 also shows that the TOOCAN algorithm is able to aggregate individual convective cells belonging to the same convective organization in a single image (example of MCS B at 1200 UTC). Finally, the new tracking algorithm segments small MCSs (MCSs D, E, and F at 1530 UTC and 1800 UTC), which cannot be identified by the "area-overlapping" technique due to the area criteria set at 5000 km^2 inherent to this methodology. Nevertheless, these systems are of special interest because they were penetrated by research aircraft for microphysical measurements during the African monsoon multidisciplinary analyses (AMMA) campaign in 2006 [5].

MCS A identified by the TOOCAN algorithm and MCS no. 1 identified by the "area-overlapping" method are then selected for a graphical representation. The temporal evolution of their areas and the temporal evolution of their propagation speeds are analyzed and compared. The propagation speed of the convective systems is here defined as the displacement of the center of gravity of the MCS. Fig. 9(a) shows that several split and merge events occur along the life cycle of MCS no. 1 processed by the "area-overlapping" tracking algorithm. Although the time evolution of this area is noisy, the MCS no. 1 describes a growing phase from 1300 UTC to 1800 UTC and then reaches the area of about 160 000 km^2. The decrease of the area is

This article has been accepted for inclusion in a future issue of this journal. Content is final as presented, with the exception of pagination.

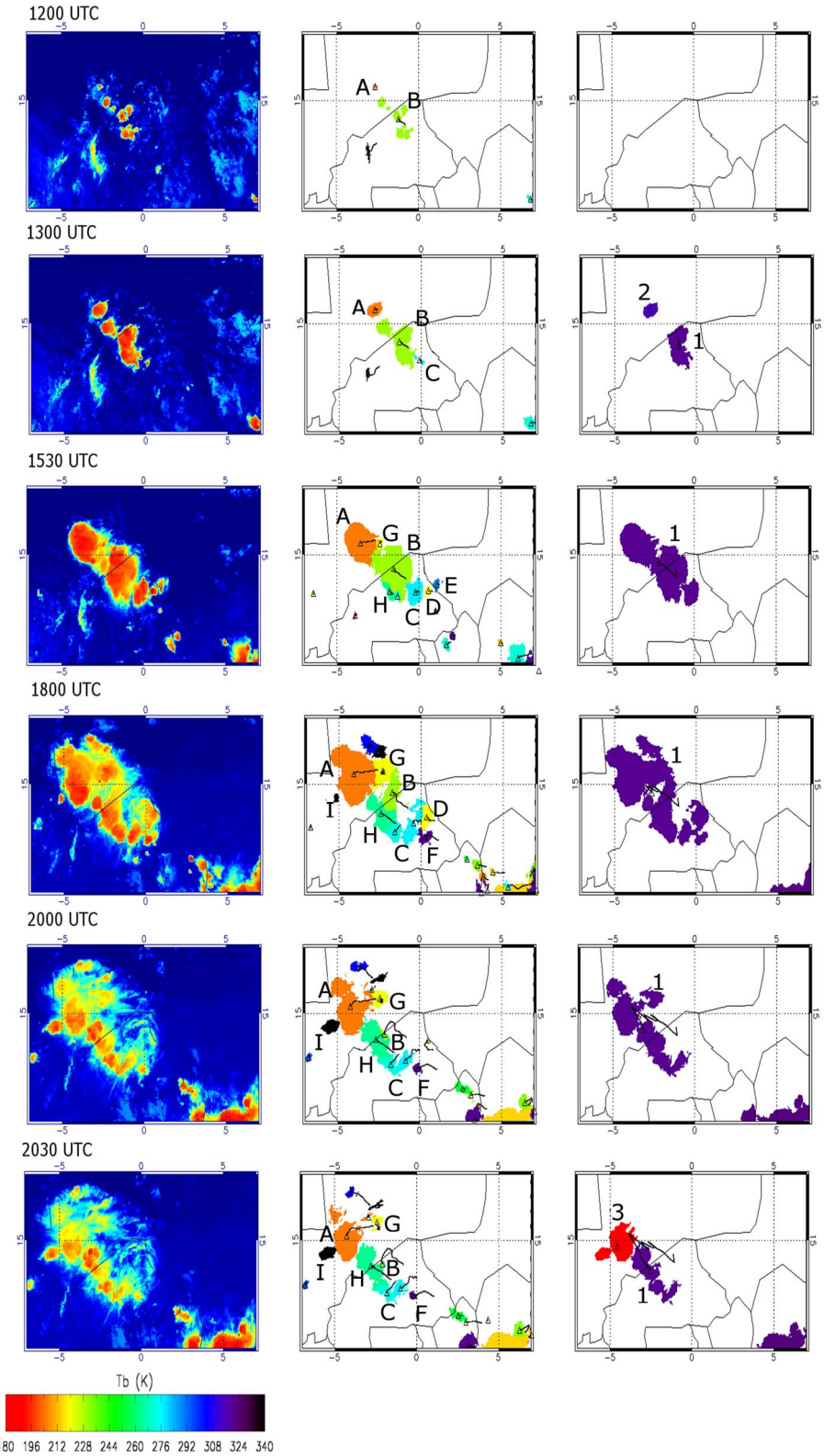

Fig. 8. Illustration of the TOOCAN and "area-overlapping" segmentations for a convective situation which occurred in September 11, 2006, over the region of Niamey. (From left to right) Time series of brightness temperature images from SEVIRI/MSG-1, time series of images corresponding to the output of the TOOCAN algorithm, and time series of images corresponding to the output of the "area-overlapping" tracking algorithm.

marked by several splits. The evolution of the MCS A is also described by a growing phase from 1300 UTC to 1900 UTC, but the surface reached (79 000 km^2) is smaller than the MCS processed by the overlapping tracking algorithm (162 000 km^2). This is explained because the TOOCAN algorithm has decomposed the cold cloud shield defined at a 235-K threshold into many objects. The MCS A then decreases until 0200 UTC on September 12, 2006.

The area evolution of MCS A is smooth because no split or merge events take place with the TOOCAN approach. On

This article has been accepted for inclusion in a future issue of this journal. Content is final as presented, with the exception of pagination.

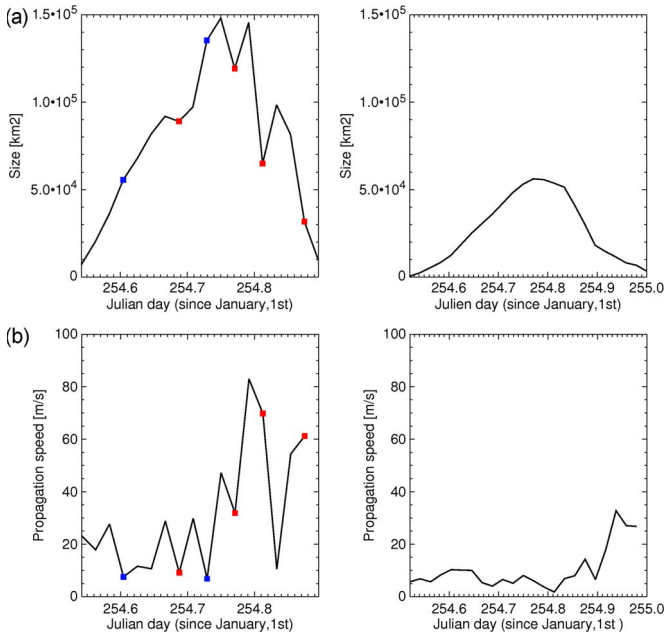

Fig. 9. (a) Evolution of the cold cloud shield associated to (right) MCS A processed by the new algorithm and to (left) the MCS no. 1 processed by the area-overlapping algorithm. Red points and blue points indicate split and merge events, respectively. (b) Evolution of the propagation speed of (right) MCS A processed by the TOOCAN algorithm and (left) MCS no. 1 processed by the "area-overlapping" algorithm. Red points and blue points indicate split and merge events, respectively.

the contrary, the propagation speed of MCS no. 1 processed by the "area-overlapping" technique presents abrupt variations [Fig. 9(b)]. Propagation speed of the center of gravity of MCS no. 1 can reach 60 m/s along its life cycle. These strong variations are explained by successive merge or split events and do not correspond to the actual propagation of the storms. If we consider the MCS A processed by the TOOCAN algorithm, we can observe that the propagation speed varies slightly, with a peak at 26 m/s and an average value of 8 m/s.

2) Bay of Bengal: Fig. 10 shows the comparison of the tracking results over a selection of images for a convective situation which occurred over the Bay of Bengal in November 10 and 11, 2011. This analysis makes use of data from the 10.8-μm infrared channel from the Meteosat Visible and InfraRed Imager (MVIRI)/METEOSAT-7 (5 km; 30 min).

First, if one considers the MCS B identified by TOOCAN, we can observe that the system is composed of a unique convective core associated to a stratiform part in the spatiotemporal domain. The TOOCAN algorithm then detects MCSs fitting the definition of a convective system given previously. As observed for the West African case study, the TOOCAN method slices up the high cloud shield in individual MCSs and does not give rise to unphysical split and merge artifacts. It is also interesting to compare the results of the two tracking algorithms at 1130 UTC corresponding to the dissipation stage of the convective situation. Indeed, between 0900 UTC and 1130 UTC, the MCS no. 2 detected by the "area-overlapping" algorithm splits in several parts yielding artificially new MCSs (MCSs no. 6–7–8–9–10–11). On the contrary, the continuity of the tracking for the MCSs identified by the TOOCAN method is maintained during the dissipation stage, as we can observe with MCSs B, D, E, and F between 0900 UTC and 1130 UTC. The new method then permits a characterization of MCSs all along their life cycles in better agreement with the actual synoptic conditions seen in the raw imagery.

3) Brazil: To complete the evaluation of the TOOCAN method over the tropics, the images from the imager instrument (IM-Imager) onboard Geostationary Operational Environmental Satellite (GOES)-12 (4 km; 15 min) for the November 2, 2011, have been processed over the region of Belem in Brazil.

The cold cloud shield is decomposed in several and individual MCSs by the TOOCAN algorithm in the spatiotemporal domain, and Fig. 11 shows that the MCS D identified by the TOOCAN algorithm consists in a convective core associated to a stratiform anvil in the spatiotemporal domain. As previously observed over the other tropical regions, the MCSs detected by the TOOCAN algorithm over the Brazilian region then still fit the definition of MCS given previously. This case study shows also the capability of the TOOCAN algorithm to detect small MCSs, in particular at 0230 UTC and 1545 UTC, which cannot be identified by the "area-overlapping" method due to the minimum size criteria set at 5000 km^2. Over this tropical region, the detection of small MCSs is of utmost importance. Indeed, a large population of MCSs has short lifetime duration [28].

The analysis of these case studies illustrates the problems due to merges and splits which can be generated artificially by the overlap-based tracking algorithm. It has also underlined the capacity of the TOOCAN algorithm to tackle these problems and to improve the MCS segmentation, for different tropical regions or organized convective situations, allowing a coherent characterization of MCSs along their life cycle.

B. Statistical Analysis

In this section, the statistical analysis aims to measure the importance of the problems generated by the unphysical splits and merges affecting the MCSs identified by the "area-overlapping" methodology. Thus, the improvements brought by the TOOCAN algorithm on the description of convective system life cycles could be quantified. The analysis is conducted over the West African region for the whole month of July 2006. Over this period and this region, the TOOCAN algorithm identifies around 17 500 MCSs, while the number of MCSs segmented by the "area-overlapping" technique is five times less (around 3500). Similarly, the total cold cloudiness identified by TOOCAN reaches 2.14×10^9 km^2 and is 1.25 times larger than those detected by the "area-overlapping" algorithm. Moreover, 50% of the MCSs identified by the "area-overlapping" algorithm (contributing to more than 66% of the total cold cloudiness) are affected by split and merge events. Fig. 12(a) shows the population of MCSs identified by the TOOCAN and the "area-overlapping" algorithms according to their lifetime durations. The distribution of the MCSs segmented by the "area-overlapping" algorithm and describing a "clean" and complete life cycle (with no split and merge events) is also shown. Both of the distributions decrease according to the increase of the lifetime duration. However, for the 2–20-h lifetime interval, the distribution shows a larger population of MCSs segmented by TOOCAN than for the other algorithm. The maximum of population is reached for the TOOCAN algorithm for the 2–4-h interval, with around 3500 MCSs segmented, and for the

This article has been accepted for inclusion in a future issue of this journal. Content is final as presented, with the exception of pagination.

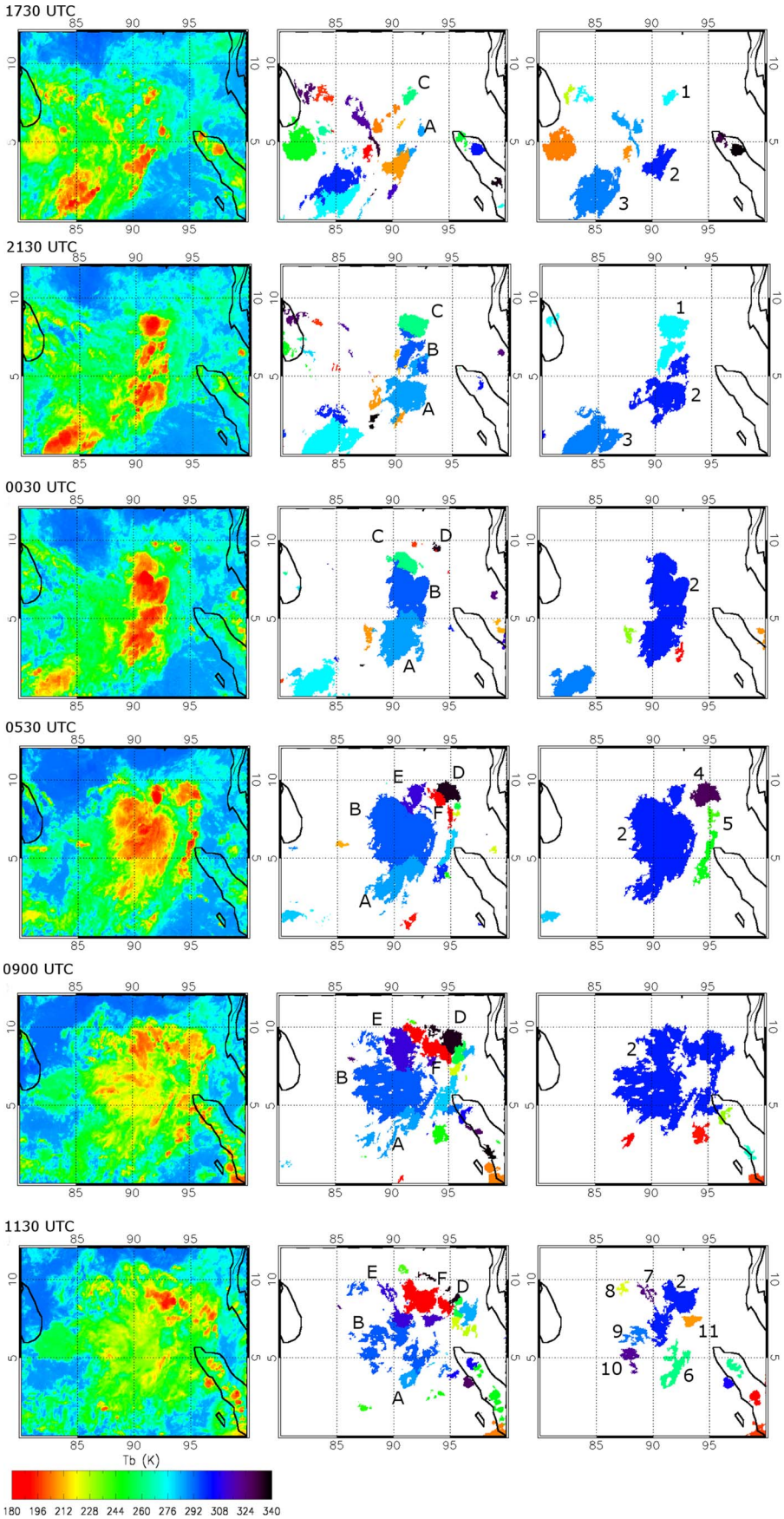

Fig. 10. Illustration of the TOOCAN and "area-overlapping" segmentations for a convective situation which occurred in November 10 and 11, 2011, over the southern part of the Bay of Bengal. (From left to right) Time series of brightness temperature images from MVIRI/METEOSAT-7, time series of images corresponding to the output of the TOOCAN algorithm, and time series of images corresponding to the output of the "area-overlapping" tracking algorithm.

This article has been accepted for inclusion in a future issue of this journal. Content is final as presented, with the exception of pagination.

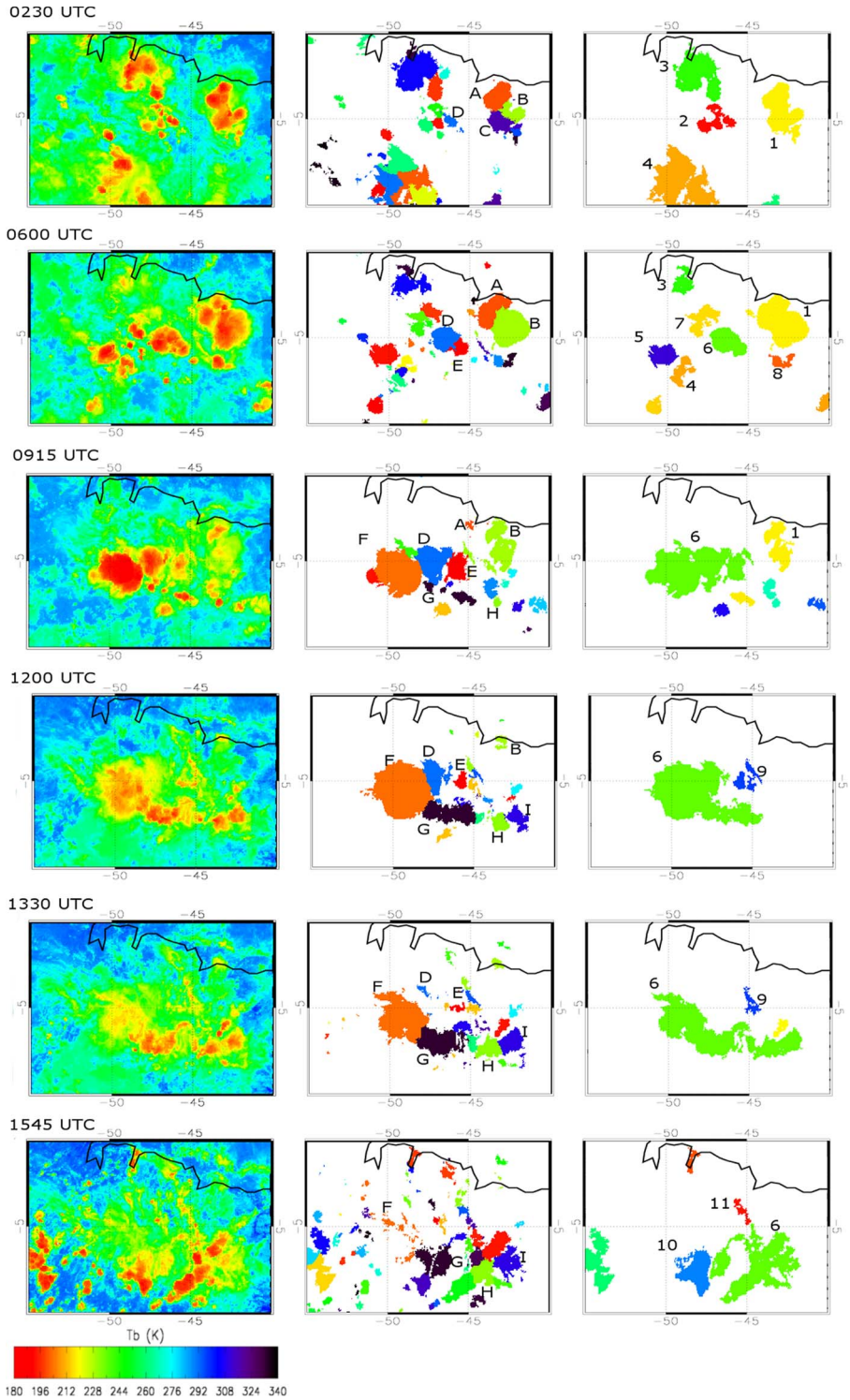

Fig. 11. Illustration of the TOOCAN and "area-overlapping" segmentations for a convective situation which occurred in November 2, 2011, over the region of Belem in South America. (From left to right) Time series of brightness temperature images from IM-Imager/GOES-12, time series of images corresponding to the output of the TOOCAN algorithm, and time series of images corresponding to the output of the "area-overlapping" tracking algorithm.

1–2-h interval for the "area-overlapping" technique. For the TOOCAN algorithm, the maximum of population is reached for the 2h-4h interval, with around 3500 MCSs segmented and for the "area-overlapping" technique, this maximum is reached for the 1h-2h interval. Over a 24-h lifetime duration, while the TOOCAN algorithm identifies only two MCSs, the "area-overlapping" algorithm segments a large number of MCSs with a lifetime greater than 24 h (27 MCSs). Four of these systems have a lifetime duration greater than two days, i.e., twice longer than that for the MCSs segmented by TOOCAN. This is explained by the multiple merging events affecting these MCSs, inducing artificial regenerations. Indeed, the distribution of MCS no split/no merge indicates that only few systems have a lifetime duration greater than 24 h. This distribution then illustrates the problems caused by the split and merge artifacts on the MCS lifetime durations.

This article has been accepted for inclusion in a future issue of this journal. Content is final as presented, with the exception of pagination.

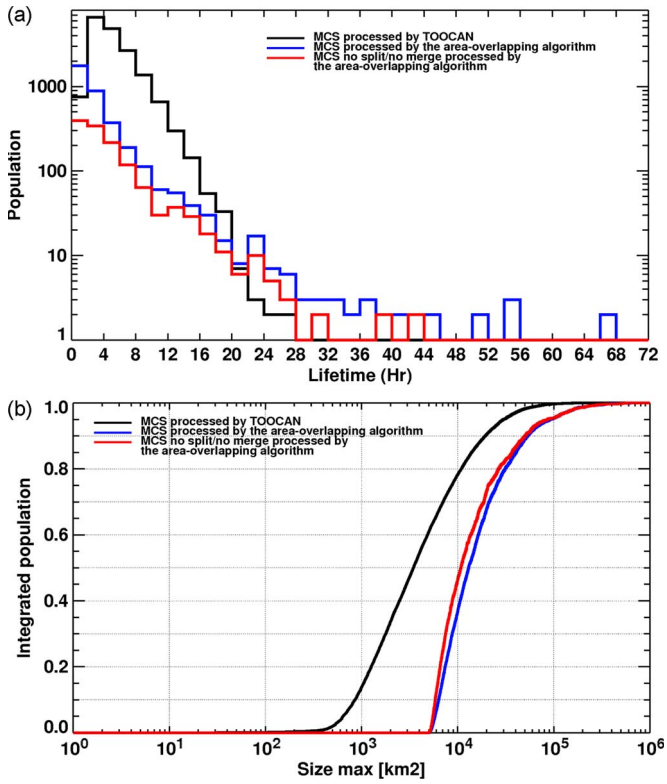

Fig. 12. (a) Distribution of the population of MCS segmented by (black) the TOOCAN algorithm and by (blue) the "area overlapping" algorithm according to the lifetime duration (in hours). The red line corresponds to the population of MCS segmented by the "area-overlapping" algorithm and which is not affected by an initiation due to a split event and by a dissipation due to a merge event. (b) Cumulated distribution function of the population of MCS segmented by (black) the TOOCAN algorithm and by (blue) the "area-overlapping" algorithm according to the maximum size (in square kilometers) reached by the MCS during their life cycle. The red line corresponds to the MCS segmented by the "area-overlapping" algorithm and which is not affected by an initiation due to a split event and by a dissipation due to a merge event.

Fig. 12(b) shows a cumulated distribution function of the MCS population segmented by the two tracking algorithms according to their maximum area (in square kilometers) reached during their life cycle. We can first notice that none of the systems detected by the "area-overlapping" technique have an area lower than 5000 km^2, which is due to the area threshold criteria set at 5000 km^2 inherent to this kind of algorithm. MCSs reaching a maximum area of 10 000 km^2 explain 50% of the total population. The filtering of MCSs describing a "clean" and complete life cycle does not strongly modify the distribution. As we have observed previously and owing to the low criteria applied for the 3-D detection step, the TOOCAN method manages to detect smaller MCSs, so that systems defined by a maximum size lower than 2000 km^2 explain 50% of the total population. However, the objective of the TOOCAN algorithm to decompose the cold cloud shield defined at a 235-K threshold in several MCSs explains the weak contribution of MCSs reaching an area greater than 100 000 km^2, while MCSs greater than this area contribute to 5% of the total population for the "area-overlapping" technique. The maximum of maximum area reached by the MCS identified by TOOCAN ($\sim$235000 km^2) is then three times smaller than those concerning the systems segmented by the "area-overlapping" technique.

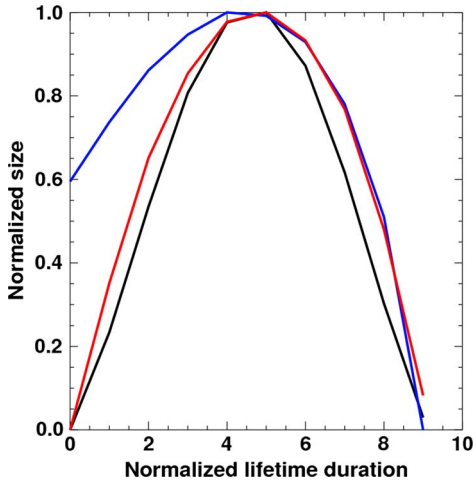

Fig. 13. Composites of the cold cloud shield associated to the MCS along their life cycle. The size is normalized between zero and one. The lifetime is normalized between zero and ten and discretized in ten steps. Black line represents the composite for the MCS segmented by TOOCAN; the blue line represents the composite for the MCS segmented by the "area-overlapping" algorithm; the red line represents the composite for the MCS no split and no merge segmented by the area-overlapping" algorithm.

Fig. 13 compares the statistical composites of the evolution of the cold surface associated to MCSs segmented by the two algorithms along their life cycles. For this, the area of each MCS is normalized between zero and one. Similarly, the lifetime duration of each MCS is normalized and discretized in ten steps. This normalized domain allows us to build an MCS composite describing the average evolution of the cold cloud shield associated to convective systems from 17 500 systems for the TOOCAN algorithm.

Results show that the average evolution of the MCSs segmented by TOOCAN is described by a linear model with an increasing phase up to the 50% of the normalized life cycle and then a decreasing phase up to the dissipation of the MCS. At the beginning and the end of the life cycle composite, the average area is around zero. Concerning the average evolution of the surface of MCSs segmented by the "area-overlapping" method, we can observe that the composite describes the same evolution with the TOOCAN one. However, the beginning of the normalized life cycle is characterized by a normalized area of 0.6. This value is explained by the numerous MCSs that initiate from a split event and, by consequence, start with an already significant cold area. By filtering MCSs describing a complete life cycle, results show that the composite is then close to the TOOCAN one. This result illustrates the impact of the split and merge artifacts on the statistical representativeness of the area evolution of MCSs along their life cycles. It also shows the capacity and the effectiveness of the TOOCAN algorithm to tackle these issues and to document the life cycle of most of the storms, while only 65% of the MCSs identified by the "area-overlapping" method are affected by the split/merge events.

VI. Summary and Discussion

A. Summary

A new tracking methodology, called TOOCAN, has been developed to detect and track MCSs using the infrared imagery from geostationary satellite over the tropics. This methodology

This article has been accepted for inclusion in a future issue of this journal. Content is final as presented, with the exception of pagination.

has been described and evaluated in this paper. The purpose of this algorithm is to overcome the main issues of existing tracking algorithms (split and merge artifacts and description of the convective organization at the "true" extent) and, also, to improve the description of the morphological parameters of MCSs along their entire life cycles. For this, the TOOCAN algorithm is based on an iterative process of segmentation in three dimensions of the infrared imagery to identify and track MCSs. The cold cloud shield defined at a 235-K brightness temperature threshold in the spatiotemporal domain is decomposed in several MCSs, and each convective system is hence defined by a convective core associated to its anvil in the spatiotemporal domain. Thus, it has been shown that this method permits the characterization of all the morphological aspects of MCSs along their entire life cycles by suppressing split and merge artifacts.

Analyses of case studies over West Africa, Bay of Bengal, and Brazil, as well as statistical analysis, have been carried out to evaluate the effectiveness of the TOOCAN algorithm. These analyses were performed via a comparison of the TOOCAN results with the outputs of a previous tracking algorithm based on an "area-overlapping" technique and a detection with a single brightness temperature threshold. Results show that, whatever the tropical region or convective situation considered, the TOOCAN algorithm decomposes the cold cloud shield defined by a 235-K threshold in the spatiotemporal domain in several MCSs, improving the description of the MCSs through their life cycles. This segmentation of the cold cloud shield seems to be in better agreement with human analysis. It appears also that the TOOCAN algorithm detects MCSs earlier in their triggering stages and later in their dissipation stages. Moreover, MCSs identified are not anymore affected by split and merge events along their life cycles. These detection and tracking improvements refine the documentation of the morphological parameters of tropical MCSs along their life cycles and permit the characterization of a larger number of systems.

B. Discussion

From an atmospheric physical process perspective, it is of utmost importance to describe the evolution of the cold cloud shield associated to MCS in order to have a better understanding of their radiative and heat budgets. Indeed, the vertical profile of net heating due to these MCSs is driven by the relative contribution of the convective and stratiform processes to the whole cloud system [19]. The convective/stratiform fraction within a cloud system hence determines, to a large extent, its effect onto its environment. It further provides the physical link between the internal system dynamics and the impact onto its larger scale environment. The recent depiction of the evolution of the precipitating characteristics as well as the convective/stratiform fraction along the life cycle of convective systems based on the merging of MCS morphology with Low Earth Orbit satellite measurements [11], [13], [20], [22] is renewing our conceptual model of the life cycle of storms in the tropics. With the improvements brought by the TOOCAN algorithm, it will be possible to further support these kinds of studies by analyzing the behavior of a large population of MCS, without any filtering due to split and merge artifacts [12].

From a meteorological perspective, convective systems are atmospheric events, which can have natural hazard consequences, such as strong wind drafts, lightnings, heavy rainfalls, hail, and floodings. Knowledge of the convective system life cycle is then of fundamental importance, particularly in the tropics, to improve forecasting and to reduce vulnerability to extreme weather damage. Efforts have been made to elaborate algorithms for forecasting convective systems [44]. These algorithms are based on a tracking module and a forecasting module. However, the forecasting results are directly dependent on the quality of the tracking outputs and so are affected by the split and merge artifacts. Although the TOOCAN algorithm has been developed in a climatology perspective, this methodology, with some reconsiderations and modifications to deal with the real-time problematic, could also bring in some improvements to the forecasting issues. Current efforts are geared toward this endeavor at Centro Nacional De Monitoramento e Alertas de Desastres Naturais [12].

ACKNOWLEDGMENT

This work was carried out under the Megha-Tropiques mission by the CNES and CNRS. The authors would like to thank the the Institut Pierre et Simon Laplace for the computing support of the server Climserv, J. Aublanc for the support with the tracking computations, and two anonymous reviewers for their comments which have greatly helped in finalizing this paper.

REFERENCES

[1] Y. Arnaud, M. Desbois, and J. Maizi, "Automatic tracking and characterization of African convective systems on Meteosat pictures," *J. Appl. Meteorol.*, vol. 31, no. 5, pp. 443–453, May 1992.

[2] C. I. Aspliden, Y. Tourre, and J. B. Sabine, "Some climatological aspects of West African disturbance lines during GATE," *Mon. Weather Rev.*, vol. 104, no. 8, pp. 1029–1035, 1976.

[3] G. M. Barnes and K. Sieckman, "The environment of fast- and slow-moving tropical mesoscale convective cloud lines," *Mon. Weather Rev.*, vol. 112, no. 9, pp. 1782–1794, 1984.

[4] E. Boer and V. Ramanathan, "Lagrangian approach for deriving cloud characteristics from satellite observations and its implications to cloud parameterization," *J. Geophys. Res.*, vol. 102, no. D17, pp. 21 383–21 399, Sep. 1997.

[5] D. Bouniol, J. Delanoë, C. Duroure, A. Protat, V. Giraud, and G. Penide, "Microphysical characterization of West African MCS anvils," *Q.J.R. Meteorol. Soc.*, vol. 136, no. S1, pp. 323–344, Jan. 2010.

[6] L. M. V. Carvalho and C. Jones, "A satellite method to identify structural properties of mesoscale convective systems based on the Maximum Spatial Correlation Tracking Technique (MASCOTTE)," *J. Appl. Meteorol.*, vol. 40, no. 10, pp. 1683–1701, Oct. 2001.

[7] M. Desbois, T. Kayiranga, B. Gnamien, S. Guessous, and L. Picon, "Characterization of some elements of the Sahelian climate and their interannual variations for July 1983, 1984 and 1985 from the analysis of METEOSAT ISCCP Data," *J. Clim.*, vol. 1, no. 9, pp. 867–904, Sep. 1988.

[8] A. Diongue, J. P. Lafore, J. L. Redelsperger, and R. Roca, "Simulation at cloud and synoptic scales of the whole life cycle of a West African squall-line observed during HAPEX-Sahel: Validation and scales interactions," *Q. J. R. Meteorol. Soc.*, vol. 128, pp. 1899–1928, 2002.

[9] M. J. Dixon and G. Wiener, "TITAN: Thunderstorm identification, tracking, analysis, and nowcasting—A radar-based methodology," *J. Atmos. Ocean. Technol.*, vol. 10, no. 6, pp. 785–797, Dec. 1993.

[10] R. M. Endlich and D. E. Wolf, "Automatic cloud tracking applied to GOES and METEOSAT observations," *J. Appl. Meteorol.*, vol. 20, no. 3, pp. 309–319, Mar. 1981.

[11] T. Fiolleau and R. Roca, "Composite life cycle of tropical mesoscale convective systems from geostationary and low earth orbit satellites observations: Method and sampling considerations," *Q. J. R. Meteorol. Soc.*, 2012, submitted for publication.

[12] T. Fiolleau, R. Roca, D. Vila, L. A. Machado, and C. F. Angelis, "A new methodology for the detection and tracking of mesoscale convective

This article has been accepted for inclusion in a future issue of this journal. Content is final as presented, with the exception of pagination.

systems in the tropics using geostationary infrared data," *Geophys. Res. Abstr.*, vol. 14, p. EGU2012-11283, 2012.
[13] J. M. Futyan and A. D. Del Genio, "Deep convective system evolution over Africa and the Tropical Atlantic," *J. Clim.*, vol. 20, no. 20, pp. 5041–5060, Oct. 2007.
[14] L. Han, S. Fu, L. Zhao, Y. Zheng, H. Wang, and Y. Lin, "3D convective storm identification, tracking, and forecasting an enhanced TITAN algorithm," *J. Atmos. Ocean. Technol.*, vol. 26, no. 4, pp. 719–732, Apr. 2009.
[15] K. I. Hodges, "A general method for tracking analysis and its application to meteorological data," *Mon. Weather Rev.*, vol. 122, no. 11, pp. 2573–2586, 1994.
[16] K. I. Hodges and C. D. Thorncroft, "Distribution and statistics of African mesoscale convective weather systems based on the ISCCP Meteosat imagery," *Mon. Weather Rev.*, vol. 125, no. 11, pp. 2821–2837, Nov. 1997.
[17] R. A. Houze and A. K. Betts, "Convection in GATE," *Rev. Geophys. Space Phys.*, vol. 19, no. 4, pp. 541–576, Nov. 1981.
[18] R. A. Houze, "Cloud clusters and large-scale vertical motions in the tropics," *J. Meteorol. Soc. Jpn.*, vol. 60, no. 1, pp. 396–410, Feb. 1982.
[19] R. A. Houze, "Mesoscale convective systems," *Rev. Geophys.*, vol. 42, no. 4, pp. RG4003-1–RG4003-43, Dec. 2004.
[20] T. Inoue, D. Vila, K. Rajendran, A. Hamada, X. Wu, and L. A. T. Machado, "Life cycle of deep convective systems over the Eastern Tropical Pacific observed by TRMM and GOES-W," *J. Meteorol. Soc. Jpn.*, vol. 87A, pp. 381–391, 2009.
[21] J. T. Johnson, P. L. Mackeen, A. Witt, E. D. Mitchell, G. J. Stumpf, M. D. Eilts, and K. W. Thomas, "The storm cell identification and tracking algorithm: An enhanced WSR-88D algorithm," *Weather Forecast.*, vol. 13, no. 2, pp. 263–276, Jun. 1998.
[22] Y. Kondo, A. Higuchi, and K. Nakamura, "Small-scale cloud activity over the maritime continent and the Western Pacific as revealed by satellite data," *Mon. Weather Rev.*, vol. 134, no. 6, pp. 1581–1599, Jun. 2006.
[23] V. Lakshmanan, K. Hondl, and R. Rabin, "An efficient general-purpose technique for identifying storm cells in geospatial images," *J. Atmos. Ocean. Technol.*, vol. 26, no. 3, pp. 523–537, Mar. 2009.
[24] V. Lakshmanan, R. Rabin, and V. Debrunner, "Multiscale storm identification and forecast," *J. Atmos. Res.*, vol. 67/68, pp. 367–380, Sep. 2003.
[25] V. Lakshmanan and T. Smith, "An objective method of evaluating and devising storm-tracking algorithms," *Weather Forecast.*, vol. 25, no. 2, pp. 701–709, Apr. 2010.
[26] R. A. Maddox, "Mesoscale convective complex.," *Bull. Amer. Meteorol. Soc.*, vol. 61, no. 11, pp. 1374–1387, 1980.
[27] L. A. T. Machado, M. Desbois, and J.-P. Duvel, "Structural characteristics of deep convective systems over tropical Africa and the Atlantic Ocean," *Mon. Weather Rev.*, vol. 120, no. 3, pp. 392–406, 1992.
[28] L. A. T. Machado and H. Laurent, "The convective system area expansion over Amazonia and its relationships with convective system life duration and high-level wind divergence," *Mon. Weather Rev.*, vol. 132, no. 3, pp. 714–725, Mar. 2004.
[29] L. A. T. Machado, W. B. Rossow, R. L. Guedes, and A. W. Walker, "Life cycle variations of mesoscale convective systems over the Americas," *Mon. Weather Rev.*, vol. 126, no. 6, pp. 1630–1654, Jun. 1998.
[30] B. E. Mapes and R. A. Houze, "Cloud clusters and superclusters over the oceanic warm pool," *Monthly Weather Review*, vol. 121, no. 5, pp. 1398–1415, May 1993.
[31] D. W. Martin and A. J. Schreiner, "Characteristics of West African and East Atlantic cloud clusters: A survey from GATE," *Mon. Weather Rev.*, vol. 109, no. 8, pp. 1671–1688, Aug. 1981.
[32] V. Mathon and H. Laurent, "Life cycle of Sahelian mesoscale convective cloud systems," *Q. J. R. Meteorol. Soc.*, vol. 127, no. 572, pp. 377–406, Jan. 2001.
[33] F. Meyer and S. Beucher, "Morphological segmentation," *J. Vis. Commun. Image Represent.*, vol. 1, no. 1, pp. 21–46, Sep. 1990.
[34] C. Morel, C. Orain, and S. Sénési, "Automated detection and characterization of MCS using the METEOSAT infrared channel," in *Proc. Meteorol. Satell. Data Users Conf.*, 1997, pp. 213–220.
[35] J. L. Redelsperger, "The mesoscale organization of deep convection," in *The Physic and Parameterization of Moist Atmospheric Convection*, R. K. Smith, Ed. London, U.K.: Springer-Verlag, 1997, pp. 159–160.
[36] R. Roca and V. Ramanathan, "Scale dependence of monsoonal convective systems over the Indian Ocean," *J. Clim.*, vol. 13, no. 7, pp. 1286–1298, Apr. 2000.
[37] R. Roca, M. Viollier, L. Picon, and M. Desbois, "A multisatellite analysis of deep convection and its moist environment over the Indian Ocean during the winter monsoon," *J. Geophys. Res.*, vol. 107, no. D19, pp. 8012-1–8012-25, Aug. 2002.
[38] R. Roca, J. C. Berges, H. Brogniez, M. Capderou, P. Chambon, O. Chomette, S. Cloche, T. Fiolleau, I. Jobard, J. Lemond, M. Ly, L. Picon, P. Raberanto, A. Szantai, and M. Viollier, "On the water and energy cycles in the Tropics," *Comptes Rendus Geosci.*, vol. 342, no. 4/5, pp. 390–402, Apr./May 2010.
[39] P. Salembier, P. Brigger, J. R. Casas, and M. Pardàs, "Morphological operators for image and video compression," *IEEE Trans Image Process.*, vol. 5, no. 6, pp. 881–898, Jun. 1996.
[40] B. P. Shukla and P. K. Pal, "A source apportionment approach to study the evolution of convective cells: An application to the nowcasting of convective weather systems," *IEEE J. Sel. Topics Appl. Earth Observ. Remote Sens.*, vol. 5, no. 1, pp. 242–247, Feb. 2012.
[41] E. A. Smith and A. V. Mehta, "The role of organized tropical storms and cyclones on intraseasonal oscillations in the Asian monsoon domain based on INSAT satellite measurements," *Meteorol. Atmos. Phys.*, vol. 44, no. 1–4, pp. 195–218, 1990.
[42] C. Thomas, T. Corpetti, and E. Mémin, "Data assimilation for convective cells tracking on meteorological image sequences," *IEEE Trans.Geosci. Remote Sens.*, vol. 48, no. 8, pp. 3162–3177, Aug. 2010.
[43] G. Tsakraklides and J. L. Evans, "Global and regional variations of organized convection," *J. Clim.*, vol. 16, no. 10, pp. 1562–1572, May 2003.
[44] D. A. Vila, L. A. T. Machado, H. Laurent, and I. Velasco, "Forecast and Tracking the Evolution of Cloud Clusters (ForTraCC) using satellite infrared imagery: Methodology and validation," *Weather Forecast.*, vol. 23, no. 2, pp. 233–245, Apr. 2008.
[45] M. Williams and R. A. Houze, "Satellite-observed characteristics of winter monsoon cloud clusters," *Mon. Weather Rev.*, vol. 115, no. 2, pp. 505–519, 1987.

Thomas Fiolleau received the M.S. degree in signal processing with a specialization in image processing from Université Paris VI, Paris, France, in 2004 and the Ph.D. degree with a thesis on the use of satellite observation to study mesoscale convective systems in the framework of the Megha-Tropiques Indo-French satellite mission from the Ecole Polytechnique, Paris, in 2010.

He was an Associate Engineer with the Laboratoire de Météorologie Dynamique (LMD), Institut Pierre et Simon Laplace, Paris, for two years. After working on a six-month postdoctoral project with LMD, he is currently a United Nations Educational, Scientific and Cultural Organization (UNESCO) Consultant with Centro Nacional de Monitoramento e Alertas de Desastres Naturais (CEMADEN), Cachoeira Paulista, Brazil, a Brazilian operational center, where he works on the forecast of tropical storms and precipitation over Brazil. His areas of specialization are remote sensing, image processing, and climatology and meteorology, and his research interests are focused on cloud detection and tracking and forecast algorithms using geostationary satellite data. This includes image processing of satellite and radar observations, as well as general interest in meteorology.

Rémy Roca received the M.S. degree in fundamental physics, with major in remote sensing, and the Ph.D. degree in 2000 with a thesis on the use of satellite observations to evaluate climate models from Université Paris 7, Paris, France.

He was with Scripps Institution of Oceanography, University of California, San Diego, for almost two years where he got familiar with image processing and cloud detection and tracking algorithms from geostationary satellites. From 2001 to 2012, he has been with the Laboratoire de Météorologie Dynamique, Institut Pierre et Simon Laplace, Paris, where he was a CNRS Researcher. He was appointed Mission Scientist of the Megha-Tropiques Indo-French satellite mission and took over the PIship of the mission in 2007. He was also the Head of the "Cycle de l'eau et de l'énergie" team. He is now a CNRS researcher with the Laboratoire d'Etudes en Géographie et Océanographie Spatiale in Toulouse. His broad interests are focused on the study of the water cycle in the tropics and the use of satellite observations to investigate the tropical variability. He has participated in the Indian Ocean Experiment campaign in 1999 and led the Paris AMMA Operational Centre during the AMMA campaign in 2006 and finally acted as a Forecaster for the French participation to the Dynamics of the Madden-Julian Oscillation experiment in late 2011. He has more than ten years of experience in the field of tropical climate, meteorology, and remote sensing. Since March 2011, he has owned an Accreditation to Supervise Research from Université Paris VI, Paris.